JAERI-M
82-213

VERTICAL POSITION CONTROL OF THE ELONGATED INTOR PLASMA

January 1983

Kojyu UEDA*, Satoshi NISHIO, Noboru FUJISAWA
Masayoshi SUGIHARA, Seiji SAITO** and
Kenro MIYAMOTO***

日本原子力研究所
Japan Atomic Energy Research Institute

JAERI-Mレポートは，日本原子力研究所が不定期に公刊している研究報告書です。
入手の問合わせは，日本原子力研究所技術情報部情報資料課（〒319-11茨城県那珂郡東海村）あて，お申しこしください。なお，このほかに財団法人原子力弘済会資料センター（〒319-11 茨城県那珂郡東海村日本原子力研究所内）で複写による実費頒布をおこなっております。

JAERI-M reports are issued irregularly.
Inquiries about availability of the reports should be addressed to Information Section, Division of Technical Information, Japan Atomic Energy Research Institute, Tokai-mura, Naka-gun, Ibaraki-ken 319-11, Japan.

編集兼発行　日本原子力研究所
印　　刷　㈱高野高速印刷

JAERI-M 82-213

Vertical Position Control of the Elongated INTOR Plasma

Kojyu UEDA*, Satoshi NISHIO, Noboru FUJISAWA
Masayoshi SUGIHARA, Seiji SAITO** and
Kenro MIYAMOTO***

Division of Large Tokamak Development,
Tokai Research Establishment, JAERI

(Received December 20, 1982)

Both of the shell effect due to passive shell-structures and the characteristic of simplified feedback control systems, for the vertical position stabilization of the elongated INTOR plasma, are studied and the following conclusions have been obtained.

Inductive components of the device consist of shells, shields and control coils. Both of the shells and shields are toroidally divided into 24 sectors.

A newly devised rectangular shell, which has the sufficient shell effect for the stabilization of the fast mode, is presented, along with the studies of various kinds of shell-structures described on this paper. It can be expected that the rectangular shells have negligibly small effect on the breeding ratio by locating them separately on both of the front and rear surfaces of blanket.

Some properties with the modelled feedback control system are elucidated under a disturbance field, $B_d = B_\infty \cdot [1 - \exp(-t/\tau_d)]$ (B_∞: field strength at $t = \infty$, τ_d: time constant). They are studied for two kinds of decay indices, that is, -1.0 for the pump limiter and -1.3 for the divertor. Conclusively, the control system is found to have good characteristics.

---

* On leave from MITSUBISHI Electric Co., Tokyo

** On leave from HITACHI Co., Hitachi

*** Tokyo University, Tokyo

The PID controller seems to provide the stable control of vertical position better than the PI controller.

The maximum of vertical displacement, Z_p^{max} under the disturbance field, B_d, are in proportion to B_∞. The power required for its stabilization, P, are also in proportion to B_∞^2, and then to $(Z_p^{MAX})^2$, too. Therefore, some common basis for B_∞ or Z_p^{MAX} is required for its estimation.

Moreover, the power is found to be independent of selection of the PI or PID controller, and to have approximately the same relation with Z_p^{MAX}. The difference of P between -1.0 and -1.3 in the decay index is very large when Z_p^{MAX} is more than -1.0 cm. For example, in the vicinity of Z_p^{MAX} = 1.0 cm, the power in the case of n = -1.0 is about one half of that in the case of n = -1.3. But it decreases abruptly when Z_p^{MAX} is less than 0.5 cm.

Keywords : Plasma Control , Feedback Control , INTOR ,
Plasma Position , Shell Effect , Control Power

JAERI－M 82－213

INTOR非円形プラズマの垂直位置制御

日本原子力研究所東海研究所大型トカマク開発部
上田　孝寿*・西尾　敏・藤沢　登
杉原　正芳・斉藤誠次**・宮本　健郎***

（1982年12月20日受理）

INTOR非円形プラズマの垂直位置安定化に要するシェル構成および制御系について記述する。

安定化において考慮される回路要素は，シェル構成，遮蔽体および制御コイルであり，実際の炉構成に比べて簡単化されている。

速い不安定の抑制に対して十分なシェル効果を発揮する矩形コイル状シェルの新しい型が提案されている。それは，一連のシステマティックなシェル構成の研究から生まれた。このシェル構成は，プラズマに近接して配置されるが，トリチウム増殖率への影響は無視できる程度まで軽減できることが判った。

モデル化された制御系は，外乱磁界，B_d （$=B_\infty \cdot [1-\exp(-t/\tau_d)]$）（$B_\infty$：$t=\infty$での磁界，$\tau_d$：時定数）の下で研究されている。曲率指数（n－index）は，ポンプリミター用に－1.0，ダイバータ用に－1.3，の2種類が選択されている。

結果としては，上記制御系および条件の下では，良好な特性が得られることが判った。n－index，－1.0および－1.3から得られる制御電源容量は，大きく異なる。たとえば，上記外乱の下で垂直方向の最大変位置を約1cmに抑制しようとする場合，－1.3の電源容量は，－1.0の約2倍必要となる。

＊外来研究員：三菱電気

＊＊外来研究員：日立

＊＊＊東大理学部

Contents

目　　次

1. Introduction

Both of the shell effect due to passive shell-structures and the characteristic of simplified feedback control systems, for the vertical position stabilization of an elongated plasma, are described in this paper. These studies were presented on the INTOR Workshops from the Phase I through the Phase II A.[1]∿[3],[7],[9]

The shell effect is indispensable for suppression of the fast vertical position instability with plasmas of 1.5∿1.6 in elongation. The evaluation method of shell effect in this paper is based on previous papers.[4]∿[6] Therefore, main subjects here are directed to shell-structures desirable to tokamak reactors, and three kinds of shell-structures, i.e. doughnut-like shells, cylindrical rings and rectangular coils are investigated.

The INTOR specification for the shell effect requires that the shell-structure should produce the larger growth time of vertical positional instability than 50 msec. This target on the growth time is found later to be reasonable and compatible with the stable active control of its instability, and to result in the acceptable power supply for position control, judging from some simulations with the modelled feedback control system described in this paper.

Actually shell-structures need to be toroidally divided into 24 sectors to make the remote assembly and maintenance of the torus possible. Some structures without cuts, for example, the cylindrical rings which are studied in detail, does not seem to be practical. But those studies is very useful for obtaining better shell-structures. The shell-structure should also be located as close to the plasma column as possible to assure usefull shell effect, and it is expected to be located just behind

the first wall. Additionally, its thickness should be selected to be as thin as possible, taking its influence upon the breeding ratio into account.

A new shell-structure presented here has the sufficient shell effect and just a little effect on the breeding ratio. This structure can provide the stable control not only for the pump limiter case, but also for the divertor type. The decay index of the vertical magnetic field for plasma confinement has about -1.0 for the pump limiter and about -1.3 for the divertor. The difference, 0.3 imposes more strict requirements for the shell-structure.

In this paper are also described some properties with the simplified two feedback control systems for stabilization of the slow mode with the elongated INTOR plasma. One is composed of the shell-structure, a shield structure, and a pair of control coils. Another has only shell-structures and a pair of control coils. As a sector of shells, the new type of shell-structure is employed. The PID or PI controller is used as the method of feedback control and both of the systems will be found to have good characteristics. A tentative value for disturbance field or vertical displacement is adopted for estimation of the power required for its stabilization.

The shell effect is described in Section 2 and the modelled feedback control system in Section 3. The theoretical bases of both of the shell effect and control system are provided in Section 2.1 and in Section 3.1, respectively. The shell-structures are described in Section 2.2.2 for the pump limiter, and in Section 2.2.3 for the divertor. The results and discussions for the feedback control is given in Section 3.2.2.

2. Shell Effect

2.1 Basic equations

An evaluation of shell effect is based on analyses of the interaction between a plasma column and a group of passively inductive structures surrounding the column. Therefore, its basic equations consist of the following equations. One of them is the equation of plasma motion in the cylindrical coordinates[4].

$$m_p \ddot{Z}_p = I_p \, (B_0 \cdot n/R_p) \cdot Z_p - I_p \cdot \Big(\sum_{i=1}^{N} B_i + B_d \Big) \quad , \tag{1}$$

which is based on the assumption that the plasma column behaves like a rigid column. The others are circuit equations between its column and the inductive structures,

$$\dot{I}_i + \sum_{\substack{j=1 \\ (j \neq i)}}^{N} (M_{ij}/L_i) \cdot \dot{I}_j + (R_i/L_i) \cdot I_i = -I_p \cdot [(\partial M_{pi}/\partial Z)/L_i] \cdot \dot{Z}_p \quad , \tag{2}$$

where Z_p, m_p, I_p and R_p are the axial displacement, mass per unit length, current and major radius of the plasma column, respectively. B_0 and n are the axial component and n-index of the equilibrium field (Shafranov's field) at $(R_p, 0.0)$, respectively. I_i, L_i, R_i, M_{ij}, M_{pi} and B_i with the i-th inductive structure are its current, self-inductance, resistance, mutual inductances with the j-th inductive structure and with the plasma column, radial component of the magnetic field produced approximately at $(R_p, 0.0)$ by I_i. B_d is a disturbance field. $\dot{}$ means time-derivative, d/dt. Moreover, B_i is expressed by

$$B_i = \nu_i \cdot I_i \quad , \tag{3}$$

where ν_i is its radial field per unit current, approximately at $(R_p, 0.0)$.

The above inductive structures of a tokamak fusion reactor indicate a vacuum chamber, shell structure, blankets, shield and so forth. In general, an inductive structure has various kinds of inductive current components, that is, eigen modal currents which are not coupled mutually. A modal current can be dealed equivalently as one of the inductive structure on Eq.(1), Eq.(2) and Eq.(3).

Suppose a shell structure with M in number of its modal currents $(M_{ij} = 0)$. Equations from Laplace transformation of Eq.(1) and Eq.(2), using Eq.(3) and setting $B_d = 0$, give

$$\tau_0^2 \cdot \gamma_g^2 = -\left[n + \sum_{m=1}^{M} \{n_m \cdot \tau_m \cdot \gamma_g / (1 + \tau_m \gamma_g)\}\right] \quad , \tag{4}$$

where τ_0 is the intrinsic time constant of plasma column $(\equiv \sqrt{-m_p R_p / I_p B_0}$, $I_p > 0$, $B_0 < 0)$, and γ_g and τ_m are the growth rate of its vertical displacement or vertical instability and the time constant of m-th modal current, respectively. n_m is defined by

$$n_m = \nu_m \cdot [(\partial M_{pm}/\partial Z)/L_m] \cdot (R_p I_p / B_0) \quad (>0) \quad . \tag{5}$$

It is found that if $\tau_m \cdot \gamma_g \gg 1$ and $(n + \sum_{m=1}^{M} n_m) > 0$, the shell effect can be expected, and, on the other hand, if $\tau_m \cdot \gamma_g \ll 1$, no shell effect can be obtained.

In a case that the shell structure has only a modal current and B_d is given by $B_\infty \cdot [1 - \exp(-\lambda t)]$ $(B_\infty = B_d|_{t=\infty})$, an analytical solution with Z_p in Eq.(1) and Eq.(2) is given approximately by

$$Z_p = A \cdot e^{-\lambda_1 t} \cdot \sin\beta t + B \cdot e^{\lambda_2 t} + C \cdot e^{-\lambda t} + D \quad , \tag{6}$$

where both of $Z|_{t=0}$ and $\dot{Z}|_{t=0}$ are set to zero and τ_0 is assumed to be negligibly small in comparison with τ_1. Constants are defined by

$$\lambda_1 = n_1/2(n+n_1)\tau_1 \quad (>0,\ n_1>0,\ n_1>-n) \quad , \tag{7}$$

$$\lambda_2 = -n/(n+n_1)\tau_1 \quad (>0) \quad , \tag{8}$$

$$\beta = \sqrt{(n+n_1)}/\tau_0 \quad , \tag{9}$$

$$A = -(B_\infty R_p/B_0)\cdot[\lambda\tau_0/(n+n_1)^{3/2}] \quad , \tag{10}$$

$$B = -(B_\infty R_p/B_0)\cdot[\lambda n_1\tau_1/n\{\lambda\tau_1(n+n_1)-n\}] \quad , \tag{11}$$

$$C = (B_\infty R_p/B_0)\cdot[(1-\lambda\tau_1)/\{\lambda\tau_1(n+n_1)-n\}] \quad , \tag{12}$$

$$D = (B_\infty R_p/B_0 n) \quad . \tag{13}$$

The first term in Eq.(6) is produced from the term on the left hand side of Eq.(1), and is damping-oscillatory if $n_1 + n > 0$. Its second term is a diverging one with λ_2^{-1} in growth time. The larger λ_2^{-1} provides the more useful the shell effect becomes. λ_2^{-1} is found to be comparable with τ_1 because $|n| \simeq (n+n_1) \simeq 1.0$.

The ratio of $|A|$ to $|B|$ in Eq.(6) is given approximately by $(\tau_0/\tau_1)\cdot(n+n_1)^{-(3/2)}$ and is found to be negligibly small compared with 1 under the present parameters: $n = -1.0$, $n_1 = 1.50$, $\tau_0 \cong 10^{-6}$ s and $\tau_1 \cong 0.1$ s. Therefore, the left term in Eq.(1) can be neglected in comparison with its right term, and then Eq.(1) is expressed approximately by

$$Z_p = (R_p/B_0 n) \cdot \left[\sum_{i=1}^{N} \nu_i I_i + B_d \right] \quad . \tag{14}$$

Suppose a shell structure with two modal currents, in order to obtain a further more measure of shell effect for any shell structure with multi-modal currents or for multiple shell structures. In this case, two eigen values, α_m $(m = 1,2)$, corresponding to the reciprocal of each time constant for the vertical displacement can be obtained from Eq.(2) and Eq.(14), and expressed by

$$\alpha_m = \left[-n/\tau_1(n+n_1+n_2)\right] \cdot f_m(\alpha_0,\beta_1,\beta_2) \quad , \tag{15}$$

where suffix m $(m = 1,2)$ is used for the m-th mode. $f_m(\alpha_0,\beta_1,\beta_2)$ is given by

$$f_m = (1/2) \cdot \left[\alpha_0(1+\beta_1) + 1 + \beta_2\right] + (-1)^{m+1} \cdot \sqrt{\left[\alpha_0(1+\beta_1) - 1 - \beta_2\right]^2 + 4\alpha_0\beta_1\beta_2} \quad ,$$

where α_0, β_1 and β_2 is (τ_1/τ_2), (n_1/n) and (n_2/n), respectively. In case of $\tau_1 = \tau_2 = \tau_c$, Eq.(15) is reduced as follows, taking $\beta_1 < 0$ and $\beta_2 < 0$ into account.

$$\alpha_1 = -n/\tau_c(n+n_1+n_2) \tag{16}$$

$$\alpha_2 = -1/\tau_c \tag{17}$$

Therefore, the shell effect in $\tau_1 = \tau_2$ is found to be expressed by α_1 and to have $(n+n_1+n_2)$ as its measure, and, in general, it can be estimated by $n + \sum_{m=1}^{M} n_m$ in case of multi-modal currents with $\tau_1 = \tau_2 --- = \tau_M$.

On the other hand, α_1, in case of $\tau_1 \neq \tau_2$, can be known from Fig.1, where dependence of $f_1(\alpha_0,\beta_1,\beta_2)$ upon α_0^{-1} is shown on selecting typical sets of

(β_1,β_2). It is found that $f_1(\alpha_0,\beta_1,\beta_2)$ decreases moderately with increasing α_0^{-1} $(= \tau_2/\tau_1)$, and then decreases monotonically with decreasing $|\beta_1|$ and increasing $|\beta_2|$, too.

Suppose a case of $\beta_1 = -1.0$ and $\beta_2 = -0.75$, for example, $n = -1.50$, $n_1 = 1.50$, $n_2 = 1.13$ and $\tau_1 = 100$ ms. It gives 1.0 and about 0.6 in f_1 for 1 and 4 in α_0^{-1}, respectively. This means that this increase in α_0^{-1} gives α_1^{-1} more than in case of $\alpha_0^{-1} = 1$, by 1.67 $(= 1/0.6)$ times. That is, if one want to increase α_1^{-1} with fixed τ_1, α_1^{-1} can be fairly increased by selecting τ_2 more largely, as described on the following section.

2.2 Studies of passive shell structure

2.2.1 Plasma parameters and analysis method

The typical plasma parameters of INTOR are shown in Table 1. The negative decay index of the elongated plasma, which mainly causes unstable vertical motion, is -1.30 for the divertor and -1.0 for the pump limiter, and then the divertor is required more shell effect than the pump limiter. Additionally, the above decay index values for the divertor and pump limiter are based on typical results from the plasma equilibrium calculations. In special, the results for divertor are shown in Fig.3. It is found that 1.3 in absolute n-index is an average value, that is, smaller than the minimum from the INTOR "Universal" and larger than the maximum from the INTOR-J "Universal".

On the other hand, n_m, as defined in Eq.(5), is in proportion to the reciprocal of B_0. B_0^{-1} for the divertor is larger than for the pump limiter, and n_m obtained from one shell structure is only a little larger for the divertor than for the pump limiter.

Analyses of the shell effect consist of the following process.

(1) The eddy current evaluation from a model, in which the modal current analysis based on the finite element circuit method is used.[5] The eigen modes of current induced on a shell structure can be calculated by higher order, using its model. Here, only the largest eigen mode among those time constants is tentatively used on evaluating the positional stability.

(2) Evaluation of the derivative of its mutual inductance of the plasma column, $(\partial M_{ps}/\partial Z_p)$(s is the largest of those time constants), which is performed by both means of the dipole current model and a method using the plasma equilibrium codes.

On the dipole current model, coupling of a shell current with a plasma column is replaced by coupling of its current with a set of dipole ring currents located at $(R_p, \pm (\pi/4)a)$. $\partial M_{ps}/\partial Z_p$ in its model can be given approximately by the following equation.

$$\partial M_{ps}/\partial Z_p = (2/\pi a) \cdot M_{ds}$$
$$= (1/2) \cdot (\partial M_{ds}/\partial Z_p)$$

where M_{ds} is the mutual inductance between the shell and dipole currents. The method from the plasma equilibrium codes is due to a conventional evaluation of the mutual inductance of its column with a pair of filament currents located instead of the shell current.

In Fig.2 are shown the structural view around the plasma column, two contours, that is, contour I and II along which the shell structures or the filament current are located. The contour I is exactly located upon the first wall surface, and the contour II is located between the blanket and the shield.

In the pump limiter case, the sufficient shell effect for stabilization

of the fast mode of vertical motion is obtained by a special shell structure merely located on the top and bottom of the contour I, as shown later. On the other hand, the shell structure for divertor need to be located not only on the contour I, but also on the contour II, because of its large n-index, as shown in Table 1.

2.2.2 Shell-structure on the contour I

It is useful to get what shape of the shell-structure is preferable in obtaining the large shell effect. The four kinds of the shell-structures shown in Fig.4 are investigated.

(a) Doughnut without cuts

This is the ideal shell-structure which surrounds the plasma column, and has the best performance as the shell.

(b) Doughnut with cuts

The doughnut-like shell is devided into 24 sectors in toroidal direction. Each sector is completely insulated or connected by bellows. This has the best shell performance among the shell-structures with cuts.

(c) Plane ring with and without cuts

The shell-structure consists of a plane ring surrounding the outboad side of the plasma column.

(d) Rectangular coils

Twenty-four coils are installed on the outboard side along the circuits which will carry the first eigen mode of the doughnut with cuts. This will be the most preferable with respect to the breeding ratio and the assembly and maintenance of the device, if this shell-structure can has the sufficient shell effect.

n_s obtained from those shell structures are listed in Table 2. The dimensions of the shell-structure are shown in Fig.5(a).

The ideal shell-structure of the case (a) perhaps gives the maximum n_s and, as a matter of course, is expected to have the adequate shell effect. The plane ring without cuts placed only on the outboard, which is called (c'), is also expected to provide the enough shell effect as well as the case (a).

On the contrary, the shell-structures with cuts have the poor shell effect. Even though the shell-structures with cuts, that is, the cases (b) and (b') completely surround the plasma column, which are expected to be the best performance among those with cuts, n_s becomes less than one, and the insufficient shell effect can be provided. This poor shell effect of the shell-structures will be attributed to the fact that the first eigen mode of the induced current changes from the current in the toroidal direction to the saddle-type current.

Judging from the results in Table 2, the shell-structures with cuts seem to be unsuitable for the sufficient shell effect.

In the above, the time constant of the shell-structure, τ_s has not been discussed. In the tokamak devices in which plasma currents are induced by means of the current transformer, there is the lower limit in the loop resistance, e.g., a few tenth mΩ. It means that there is found to be the upper limit in τ_s.

The shell-structure with rings, which are shown in Fig.5, will have some difficulties in the assembly and maintenance of the torus accompanied with them. However some improvements can be expected in the breeding efficiency. The results of the typical cases are in Table 3. All cases have $n_s > 1$ and the shell effect decreasing moderately from the case (a) to the case (f) can be anticipated.

As shown in Table 1, the decay indexes, n for the divertor and pump limiter are about -1.30 and -1.0, respectively. The cases (e) and (f) are expected to be hopeful candidates for the shell structure providing the sufficient breeding ratio. Therefore, as far as on attaching important to the breeding ratio, the shell-structure shown in Fig.5 will perhaps give only the unsufficient shell effect for the divertor , and then , its studies for the divertor will be performed on taking the contour I and II shown in Fig.2 into account.

Before those studies with the shell structure adequate to the divertor, the cases (e) and (f) are investigated from the viewpoint of increasing the breeding efficiency in more detail.

The results of the case (e) and (f) are shown in Fig.6 and Table 4. The figure shows the loop resistance, R_s, and τ_s versus the thickness of the ring plate, t, with a parameter of the width of the ring plate, L. Since the growth time of the positional instability, α_s^{-1} ($\doteqdot \gamma_g^{-1}$) depends on both of τ_s and n_s of the induced current, as known from Eq.(8), the table indicates that the longer τ_s does not always suppress the vertical motion of the plasma column during the longer time span.

The case (f.1.3) can stably maintain the plasma column almost during the same time span as the case (e.1.1). When the blanket on the inboard side is non-breeding type, the case (e.1.1) is more preferable than the case (f.1.3).

In the above descriptions, the shell structures from the following points of view have been discussed.

(1) Doughnut-like shells with and without cuts, and rectangular coils as a special case of its shell with cuts.

(2) The shell-structure with some rings which are located on the contour I, and go around in the toroidal direction.

In the case (1), difference in n_s between "without cuts" and "with cuts" is found to be remarkably large. This comes from increase of L_s, and decrease of $(\partial M_{ps}/\partial Z_p)$ and ν_s due to the change of toroidal mode current to saddle-like current. On the other hand, the case of the rectangular coils has the feature that L_s is about 2.5 times as large as on the plane ring without cuts and both of $(\partial M_{ps}/\partial Z_p)$ and ν_s is only a little less than on it. That is, the decrease on both of $(\partial M_{ps}/\partial Z_p)$ and ν_s in the cases, "with cuts" is due to decrease of the toroidal component of eigen mode current, and this can be understood from the above result with the rectangular shell.

On the other hand, the case (f.1.3) in the above case (2) has the feature that L_s is about 1.7 times as large as the plane ring without cuts and both of $(\partial M_{ps}/\partial Z_p)$ and ν_s are about 1.5 times as large as the doughnut-like shell without cuts. Therefore it is clear that the above difference in L_s between the rectangular shell and the case (f.1.3) will be produced by two poloidal bars, which are the two sides of a rectangular shell from the top over bottom of the torus. The difference in both of $(\partial M_{ps}/\partial Z_p)$ and ν_s between the case (f.1.3) and the doughnut-like shell without cuts is also produced by localizing the broad toroidal current on the doughnut-like shell, usefully upon the shell in the case (f.1.3).

Figure 7 shows dependence of $(\partial M_{ps}/\partial Z_p)$ upon the location of filament current along the contour I, obtained from the equilibrium codes. The shell in the case (f.1.3) is located nearly from No.8 to No.11 in the number of filament coil position in the figure. Its location of the case (f.1.3) is found to be near the optimum region. One of 24 rectangular shells obtained on the basis of the above results is shown in Fig.8.

Figure 8 includes the dimension of structure, too, and it has about 1.0 cm (τ_s = 126 msec) in uniform thickness of copper.

These 24 rectangular shells have almost the same n_s as with (f.1.3) in Table 4 but can have the desirable τ_s by selecting a appropriate value in its thickness. Two toroidal bars at its top and bottom, which have about 1 m in width of the poloidal direction, have to be kept in its thickness as thin as possible, because of making the breeding ratio more preferable. From both of the purposes to obtain its thinner toroidal bars and to produce more effective shell effect for the divertor, will be studied some shell structures located on the contour II.

On the practical use, the shell structures on the contour I and II will synthetically have the shell effect expressed approximately on α_1 in Eq.(17) whose suffixs, 1 and 2 are used for the shell structures on the contour I and II, respectively.

2.2.3 Shell-structure on the contour II

Figure 9 shows four kinds of shell-structures located on the coutour II. All kinds of the shell-structures are devided into 24 sectors along toroidal direction, and each of the sectors has the similar structure, as shown in Fig.8.

Figure 9(a) is the ideal case, in which the plasma column is surrounded completely, and could give the best shell effect among those in Fig.9. n_2, which is shown together in the figure, is corresponding to n_s in the above section. n_2 of Fig.9(a), (b), (c) and (d) are 1.71, 1.20, 1.05 and 1.13, respectively. The case (d), similar to (f.1.3) in Table 4, is selected as the shell-structure located on the contour II, because (a) and (b) can not provide the access area of the divertor or pump limiter.

Table 5 indicats the growth time, α_1^{-1} of the plasma column for the shell-structures located simultaneously on both of the contour I and II. These shell-structures consist of the case of (f.1.3) on the contour I

and the case in Fig.9(d) on the contour II. The mutual inductance between these structures is calculated to be about 10 μH. It is found that the case of 25 ms in τ_1 produces smaller growth rate than $(1/50)(ms^{-1})$ for selection of τ_2 more than 250 ms. 25 ms in τ_1 is equivalent to about 2.6 mm (Cu) in thickness of the toroidal bars. If these cases, 250 or 500 ms in τ_2 cannot give the stable control of the vertical positional motion, any cases more than 50 ms in τ_1 will have to be selected for parameters of the shell-structures. In such cases, the influence of the thickness of toroidal bars upon the breeding ratio could not be perhaps ignored.

3. Vertical Position Control

3.1 Basic equations

The basic equations, which describe with the vertical position control of a plasma column, are given by both of Eq.(14) and the modified circuit equation from Eq.(2),

$$\dot{I}_i + \sum_{j=1}^{N} (M_{ij}/L_i) \cdot I_j + (1/\tau_i) \cdot I_i \quad ,$$

$$= - \dot{Z}_p \cdot [(\partial M_{pi}/\partial Z)/L_i] \cdot I_p + (V_i/L_i) \qquad (18)$$

where symbols except V_i are the same as in Section 2.1., and V_i is the applied voltage of the i-th inductive component and is defined by

$$V_i = 0 \qquad \text{for passive inductive component,}$$

$$= K \cdot \left[Z_p(t-\delta t) + T_p \cdot Z_p(t-\delta t) + (1/T_I) \int_{t_0}^{t-\delta t} Z_p dt \right] \qquad (19)$$

for active inductive component,

where the right hand side of Eq.(19) is the PID controller, K the gain, δt the dead time, t_0 the starting time of control, and T_I and T_D the time constants of integral and differential circuits, respectively. In this paper, δt and t_0 are set to zero, respectively.

Equation (14) is obtained by the postulate that an inertial term in proportion to the plasma mass in the Eq.(1) is negligibly small compared with other terms. The vertical position control of the slow mode satisfies this postulate, as known from one simplified analysis in Section 2.1.

We analyze here feedback control system consisting of three inductive components, that is, N = 3: rectangular shells, shield blocks and control coils. Both of the shells and the shields are passive inductive components, and only a pair of control coils are active inductive component. For this feedback control system the differential equation on the current of control coils, I_C, is easily obtained as follows.

$$\begin{aligned}
&\dot{I}_C - (N_C/T_C) \cdot I_C \\
&= N_C \cdot [A_C \cdot \dot{I}_S + B_C \cdot \dot{I}_X + C_C \cdot (\dot{B}_d/\nu_C)] \\
&+ N_C \cdot [D_C \cdot I_S + E_C \cdot I_X + F_C \cdot (B_d/\nu_C)] + N_C \cdot G_C \cdot \int_0^t Z_p \, dt \quad , \qquad (20)
\end{aligned}$$

where I_S and I_X are the current of the shells and shields, respectively, and $\dot{}$ indicates time derivative. The others are defined by

$$N_C = n / [n + n_C \cdot \{1 - (K_D/M'_{cp} I_p)\}] \quad , \qquad (21)$$

$$T_C^{-1} = (n_c/n)(K/M'_{cp} I_p) - (1/\tau_c) \quad , \qquad (22)$$

$$A_C = (n_c/n)(\nu_s/\nu_c)[(K_D/M'_{cp} I_p) - 1] - (M_{cs}/L_c) \quad , \qquad (23)$$

$$B_C = (n_c/n)(\nu_x/\nu_c)[(K_D/M'_{cp} I_p) - 1] - (M_{cx}/L_c) \quad , \qquad (24)$$

$$C_C = (n_c/n) \cdot [(K_D/M'_{cp} I_p) - 1] \quad , \qquad (25)$$

$$D_C = (n_c/n) \cdot (K/M'_{cp} I_p) \quad , \qquad (26)$$

$$E_C = (n_c/n) \cdot (K/M'_{cp} I_p) \quad , \qquad (27)$$

$$F_C = (n_c/n) \cdot (K/M'_{cp} I_p) \quad , \tag{28}$$

$$G_C = (K_I/L_c) \quad . \tag{29}$$

Additionally, the suffixs, c, s, x and p mean the control coils, shells, shields and plasma column, respectively. K_D and K_I are euqal to $(K \cdot T_D)$ and (K/T_I), respectively. ' indicates $\partial/\partial Z_p$.

For the stable control of the vertical position of plasma, two kinds of solutions can be obtained from Eq.(20), depending upon K_D. One is the case in which K_D is equal to zero and consequently N_C is nearly equal to 1.0. In this case, One of constraints for the stable control is expressed by $T_C > 0$ and is explicitly given by the following.

$$K \geq (n/n_c)(M'_{cp} I_p/\tau_c) \quad (\equiv K_0) \tag{30}$$

This solution is a diverging type and is adjusted by K so as to counterbalance with the diverging plasma column to the vertical direction.

Another is the case given by two constraints: $N_C < 0$ and $T_C > 0$. The former is explicitly expressed by

$$K_D \geq M'_{cp} I_p \cdot [1 + (n/n_c)] \quad (\equiv K_{DO}) \tag{31}$$

The latter, $T_c > 0$, is the same as Eq.(30). In this case of $(N_c/T_c) < 0$, the solution of Eq.(20) is an oscillatory type.

Other solutions except the above solutions may exist, but the solutions obtained from the circuit parameters in this paper seems to be limited to the above two types.

On the other hand, the power, P, required to suppress the divergence of the plasma column to the vertical direction can be expressed by

$$P \doteqdot |K \cdot Z_p + K_D \cdot \dot{Z}_p|^{max} \cdot |I_c^{max}|$$

$$\doteqdot |nL_c B_0 / \nu_c \cdot R_p| \cdot |(g_1/\tau_c) \cdot Z_p + g_2 \cdot \dot{Z}_p|^{max} \cdot |I_c^{max}| \quad , \qquad (32)$$

where g_1 and g_2 are the ratios of K to K_0, and of K_D to K_{DO}, respectively. The suffix "max" of the above notation means its maximum.

3.2 Modelled feedback control system

3.2.1 Structure and circuit parameters

The modelled systems discussed here are the following two.

(1) System with the rectangular shells located only on the coutour I

This system is composed of 24 rectangular shells, 24 sectors of shield, 24 sectors of blankets and a pair of coils. Its cross-sectional view is given in Fig.10 where the rectangular shell I and II are shown together, but only the shell I on the counter I is used here.

The control coils at the top and bottom of the torus are used to produce a horizontal control field and arranged preliminarily at the location in Fig.10. Each coil has one turn, 0.5 m × 0.5 m in cross-sectional area and they are at (3.7^m, ± 6.5^m) on the cylindrical coordinates.

A sector of the shield is divided into two pieces of inside and outside parts by the cut in Fig.10, and has about 1.0 m in thickness of stainless steel. A sector of the blanket occupies considerably spacious area in the figure, but is supposed to have only several cm in effective thickness of stainless steel. One of 24 rectangular shells is shown in Fig.8. Its dimension is given together in the figure, too, and it has about 1.0 cm (τ_{shell} = 126 msec.) in thickness of copper. The decay index, n is set -1.0 for the pump limiter.

Table 6 shows its circuit parameters with the shells, shields and

control coils. In the table the blanket is excluded, because its time constant is less than 10 msec and is roughly one order smaller than the others.

The shield current consists of many current modes, but, here, only one current mode, which has the largest derivative with the axial coordinate of the mutual inductance between the plasma and shield, is selected and indicated in the Table (6). Moreover, that modal current results in the largest mutual inductance not only between the shield and shell, but also between the shield and control coils. The shield has about 0.172 mΩ in resistance, and about 312 msec in time constant, for the modal current.

(2) System with two kinds of rectangular shells located on both of the contour I and II

This system consists of the shell-structures, located on both of the contour I and II, and two control coils. The shield included in the system (1) is excluded from it.

In this fairly simplified system, the rectangular shell I on the contour I is selected as thin in thickness of its toroidal bars as possible level. Therefore, the shell effect expected from the shell I is limited within shorter time span than one required for the INTOR specification, more than 50 ms, and then the rectangular shell II is set so as to compensate its shortage.

n_2 of the shell II is smaller than n_1 (The suffixs, 1 and 2 are used for the shell I and II, respectively), but τ_2 is selected to be one order larger than τ_1.

The positions of two control coils are optimized and selected (6.5^m, $\pm 6.5^m$) on the following bases.

(1) On taking the forbidden region for those locations into account

(2) The control power, P is assumed to have the following relation.

$$P \propto L_c/\nu_c^2 \quad , \tag{33}$$

where L_c and ν_c are the self-inductance of a control coil and magnetic flux density per its unit current, respectively.

Main analyses with this system are given the case of $n = -1.30$ for the divertor. Its circuit parameters are also shown in Table 7.

3.2.2 Results and discussions

The system (1) is studied at the beginning. Figure 11 shows its typical time variations of Z_p and the currents (I_c for a control coil, I_{shell} for the rectangular shell, and I_{shield} for the shield) under the disturbance field which is given by

$$B_d = B_\infty \cdot [1 - \exp(-t/\tau_d)] \quad , \tag{34}$$

where B_∞ is the field strength at $t = \infty$ and τ_d its time constant selected 10.0 ms. The figure is obtained from the PI controller which has 2.5×10^4 v/m in K and 6.0×10^3 v/m·sec in $K_I (\equiv K/T_I)$. The applied voltage, V_c for one of the control coils is given by $(K \cdot Z_p + K_I \cdot \int_o^t Z_p dt)$.

All of Z_p, I_c, I_{shell} and I_{shield} are damping-oscillatory. Each of $|Z_p|$ and $|I_c|$ has the maximum (defined by $|Z_p|^{MAX}$ and $|I_c|^{MAX}$, respectively) at the first peak.

On the other hand, I_{shell} has a sharp peak on the initial phase, and I_{shell} before this peak is useful for keeping the plasma column away from diverging with its initial velocity. The abrupt decrease from this peak to the first bottom is produced by coupling with the current of control coils, and such an analogous pattern is also seen in the time evolution of I_{shield} which has small shell effect in comparison with the rectangular shell.

Figure 12 shows time dependence of Z_p upon K with the PI controller. We select -0.001 T in B_∞, 10 ms in τ_d and 100 ms in τ_c (= the time constant of control coil). The time constant τ_1 of rectangular shell located on the contour I is selected to 100 ms and can produce about 50 ms in the growth time of vertical instability. The time constant τ_{shield} of shield is selected 100 msec. It is found that the time behavior of Z_p changes from a diverging oscillation to damping oscillations with increasing K. One of measures which are useful for finding this diversion point from divergence to convergence, is given by Eq.(30). The right hand side of Eq.(30) has about 4.10×10^3 v/m and the stable control of Z_p seems to be required for K several times larger than $(n/n_c) \cdot (M'_{pc} \cdot I_p/\tau_c)$.

Figure 13 shows time dependence of Z_p upon K_D ($\equiv K \cdot T_D$) for the PID controller which has 1.25×10^4 v/m in K and 6×10^3 v/m·sec in K_I. Increasing K_D, Z_p changes from damping oscillations to moderately damping veriation. One of the criteria for the stable control of Z_p in case of the PID controller is given by Eq.(31) whose right hand term has about 405 v/m/sec. Figure 14 shows time variation of Z_p with K_D as a parameter. Figure 14 is for n = -1.30, and different from Fig.13 with n = -1.0. The value of criterion from Eq.(31) is found to be clearer in Fig.14 than Fig.13.

In Figure 15 shows time variations of Z_p, with keeping $\tau_c \cdot K$ constant . There are selected three kinds of τ_c, that is, 50 ms, 100 ms and 200 ms. The variations are round to show almost the same for the three kinds, as far as $\tau_c \cdot K$ is a constant.

The following studies are for the system (2).

Figure 16 shows time variations of Z_p for three kinds of K for the PI controller in case of the system (2). The observed feature is the same as Fig.12. In this case, (n/n_c). $(M'_{pc} \cdot I_p/\tau_c)$ has about 3.24×10^3 v/m. Figure 17 also shows time variations of Z_p with K_D on the PID controller

which has 7.5×10^3 v/m in K and 6.0×10^3 v/m·sec in K_I. The right hand term on Eq.(31) has about 352 v/msec.

On a basis of the above results, the following conclusions can be drawn.

(1) The two systems are found to have good characteristics. The PID controller seems to provide the better control of vertical position than the PI controller.

(2) In PI controller, the following equation for the first peak value of Z_p, Z_p^{MAX} is hold.

$$Z_p^{MAX} = A_z \cdot B_\infty \tag{35}$$

The following equation with the first peak value of I_c, I_c^{MAX} is hold, too.

$$I_c^{MAX} = A_I \cdot B_\infty \tag{36}$$

Therefore, the power, P required to suppress and control the divergence of vertical position is given by

$$\begin{aligned} P &\fallingdotseq K \cdot Z_p^{MAX} \cdot I_c^{MAX} \quad , \\ &\fallingdotseq K \cdot A_z \cdot A_I \cdot B_\infty^2 \quad , \\ &\fallingdotseq K \cdot (A_I/A_z) \cdot (Z_p^{MAX})^2 \quad . \end{aligned} \tag{37}$$

(3) On the other hand, the power, P in case of the PID controller is represented by

$$P \fallingdotseq K_D \cdot \dot{Z}_p^{MAX} \cdot I_c^{MAX} \quad . \tag{38}$$

On a basis of a series of analyses, $\dot{Z}_p^{MAX}$ ($\fallingdotseq \dot{Z}_p/_{t=0}$) can be approximately expressed by

$$\dot{Z}_p^{MAX} \fallingdotseq (B_\infty/\tau_d) \cdot (C_1 - C_2 \ell n\ K_D) \quad . \tag{39}$$

Therefore, from Eq.(36) and Eq.(39), P is given by

$$P \fallingdotseq A_I \cdot (B_\infty^2/\tau_d) \cdot K_D \cdot (C_1 - C_2 \ell n\ K_D) \quad , \tag{40}$$

where C_1 and C_2 are positive constants independent of B_∞ and τ_d.

Fig.18 shows relations between P and Z_p^{MAX} for the system (2). Results of both of -1.0 and -1.3 in decay index are given in the figure. Additionally, the figure includes results of the PI or PID controllers, and all of the points are obtained under the disturbance field of B_∞ = -0.001 T and τ_d = 10 msec. The difference of P between -1.0 and -1.3 in n is very large when Z_p^{MAX} is more than 1.0 cm, but it decreases abruptly when Z_p^{MAX} is less than 0.5 cm. These results are thought to be produced from the reason that the shell can play decreasingly effective role with decreasing Z_p^{MAX}. This can be known from abruptly increasing power in considerably small Z_p^{MAX}. Power for the PI controllers is also found to be almost the same as one for the PID controllers in a range of Z_p^{MAX} shown in the figure.

The system (2) is composed of the least inductive components, i.e. the rectangular shells (shell-I and II) and the optimized control coils, and then it is thought of giving the least power required for the suppression and control of vertical instability in the INTOR. In practice, more inductive components than the system (2) are included and would result in more power for its suppression and control under the same disturbance field as in Fig.18.

4. Conclusions

Both of the shell effect due to passive shell-structures and the characteristic of simplified feedback control systems, for the vertical position stabilization of the elongated INTOR plasma, are studied and the following conclusions have been obtained.

Inductive components of the device consist of shells, shields and control coils. Both of the shells and shields are toroidally divided into 24 sectors.

A newly devised rectangular shell, which has the sufficient shell effect for the stabilization of the fast mode, is presented, along with the studies of various kinds of shell-structures described on this paper. It can be expected that the rectangular shells have negligibly small effect on the breeding ratio by locating them separately on both of the front and rear surfaces of blanket.

Some properties with the modelled feedback control system are elucidated under a disturbance field, $B_d = B_\infty \cdot [1 - \exp(-t/\tau_d)]$ (B_∞: field strength at $t = \infty$, τ_d: time constant). They are studied for two kinds of decay indices, that is, -1.0 for the pump limiter and -1.3 for the divertor. Conclusively, the control system is found to have good characteristics. The PID controller seems to provide the stable control of vertical position better than the PI controller.

The maximum of vertical displacement, Z_p^{max} under the disturbance field, B_d, are in proportion to B_∞. The power required for its stabilization, P, are also in proportion to B_∞^2, and then to $(Z_p^{MAX})^2$, too. Therefore, some common basis for B_∞ or Z_p^{MAX} is required for its estimation.

Moreover, the power is found to be independent of selection of the PI or PID controller, and to have approximately the same relation with Z_p^{MAX}.

The difference of P between -1.0 and -1.3 in the decay index is very large when Z_p^{MAX} is more than -1.0 cm. For example, in the vicinity of Z_p^{MAX} = 1.0 cm, the power in the case of n = -1.0 is about one half of that in the case of n = -1.3. But it decreases abruptly when Z_p^{MAX} is less than 0.5 cm.

Acknowledgements

The authors would like to express their sincere thanks to Drs. K. Tomabechi , M. Yoshikawa , K. Sako , T. Hiraoka , T. Tone , Y. Seki , and K. Tachikawa for their helpful discussion and continuing encouragement. They also wish to thank all other members of the next reactor design group in the JT-60 planning office , and Dr. A. Kameari in Mitsubishi Atomic Power Industries for useful discussion and suggestion on the design of shell structure and the development and application of computer codes.

The difference of P between -1.0 and -1.3 in the decay index is very large when Z_p^{MAX} is more than -1.0 cm. For example, in the vicinity of Z_p^{MAX} = 1.0 cm, the power in the case of n = -1.0 is about one half of that in the case of n = -1.3. But it decreases abruptly when Z_p^{MAX} is less than 0.5 cm.

Acknowledgements

The authors would like to express their sincere thanks to Drs. K. Tomabechi , M. Yoshikawa , K. Sako , T. Hiraoka , T. Tone , Y. Seki , and K. Tachikawa for their helpful discussion and continuing encouragement. They also wish to thank all other members of the next reactor design group in the JT-60 planning office , and Dr. A. Kameari in Mitsubishi Atomic Power Industries for useful discussion and suggestion on the design of shell structure and the development and application of computer codes.

Reference

(1) N. Fujisawa, et al: "Plasma Control of the next Tokamak", 3rd IAEA Technical Committee and Workshop on Fusion Reactor Design and Technology, Tokyo, 5-16 October (1981)

(2) K. Ueda, et al.: JAERI-M 9854 (1981)

(3) K. Ueda, et al.: "Shell Effect by Rectangular Coils" Group A Report Japanese Contribution for INTOR Workshop, Phase II A, Session IV March 22 - April 2 (1982)

(4) H. Yokomizo, et al.: JAERI-M 6693 (1976)

(5) A. Kameari and Y. Suzuki: JAERI-M 7120 (1977)

(6) Y. Nakamura and T. Ozeki: JAERI-M 9612 (1981)

(7) N. Fujisawa, M. Sugihara and K. Ueda: Reports of Physics Group Tasks for IAEA INTOR Workshop, Japan, JAERI Mar. 30 - Apr. 11 (1981)

(8) K. Sako, et al.: "Design Study of Swimming Pool Type Tokamak Reactor (SPTR)" J. Nucl. Sci. Technol., 19[6], 491 (1982)

(9) K. Ueda, et al.: "A Preliminary study about Vertical Position Control of the Elongated INTOR plasma", Group F Report Japanese Contribution for INTOR Workshop, Phase II A, Session V, 12-23 July (1982)

Table 1 Major Parameters of the INTOR

Major Radius , R_p (m)	5.3
Minor Radius , a_p (m)	1.2
Plasma Current , I_p (MA)	6.4
Divertor Plasma	
Elongation , K	1.6
Shafranof's Field , B_0 (T)	- 0.50
Decay Index , n	- 1.30
Pump Limiter	
Elongation , K	1.5
Shafranof's Field , B_0 (T)	- 0.52
Decay Index , n	- 1.0

Table 2 Decay Index for Shell-structure in Fig.4

Cases	n_s
(a) Doughnut without cuts	2.35
(b) Doughnut with bellows	0.73
(b') Doughnut with cuts	0.75
(c) Plane ring with cuts	0.73
(c') Plane ring without cuts	2.25
(d) Rectangular coils	0.64

Table 3 Decay Index for Shell-structure in Fig.5

Cases	(a)	(b)	(c)	(d)	(e)	(f)
n_s	2.35	2.32	1.96	2.32	1.82	1.52

Table 4 Shell Effect with Shell-structures for Cases (e) and (f) in Fig.5

Cases	R(mΩ)	L_1	L_2	τ_s(ms)	n_s	γ_g^{-1}(ms)
(e.1.1)	0.25	0.44	0.64	24	1.53	22
(e.1.2)		0.73		21	1.33	6
(e.2.1)		0.44		39	1.53	27
(e.2.2)		0.73		34	1.33	11
(f.1.1)			0.48	44	1.11	4
(f.1.2)			0.64	40	1.26	10
(f.1.3)			0.96	36	1.52	20
(f.2.1)			0.48	77	1.11	6
(f.2.2)			0.34	75	1.26	17
(f.2.3)			0.96	73	1.52	31

Table 5 Growth Time of the Plasma column from the Shell-structures located on both of the contour I and II

τ_1 (msec.)	τ_2 (msec.)	$(1/\alpha_1)$(msec.)	
		n = - 1.0	n = - 1.3
25	100	63.3	32.8
	250	101.0	46.2
	500	146.1	58.1
50	100	-	49.5
	250	-	71.0
	500	-	90.8

Table 6 Circuit Parameters

(System (1))

(μH)

i \ j	1. Shell	2. Shield	3. Coils
1. Shell	46.7	10.48	1.40
2. Shield		53.77	2.68
3. Coils			38.00
$\partial M_{pj}/\partial z(\frac{\mu H}{m})$	- 5.86	- 2.72	- 0.64
$\nu_j(10^{-7}T/A)$	1.77	0.832	0.180
n_j	1.45	0.275	0.010

(1) Plasma Parameters

I_p = 6.4 MA , B_0 = - 0.52

R_p = 5.3 m , n = - 1.0

Table 7 Circuit Parameters

(System (2))

(μH)

i \ j	1. Shell- I	2. Shell-II	3. Coils
1.Shell-I	46.7	9.96	1.51
2.Shell-II		37.2	2.40
3.Coils			47.1
$\partial M_{pj}/\partial z(\frac{\mu H}{m})$	- 5.86	- 4.62	- 0.62
$\nu_j(10^{-7}T/A)$	1.77	1.39	0.37
n_j	1.45	1.13	0.0159

(1) Plasma Parameters

I_p = 6.4 MA , B_0 = - 0.50

R_p = 5.3 m , n = - 1.30

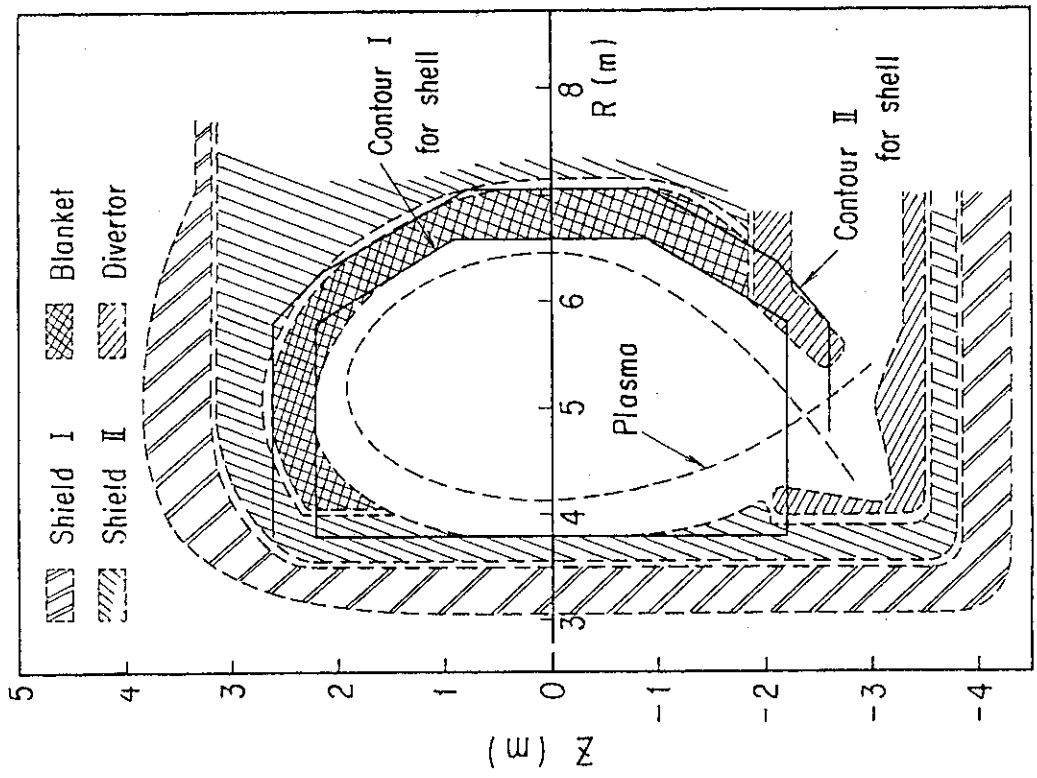

Fig. 2 Structural view nearby the plasma column, and two contours, that is, contour I and II along which shell-structures are located

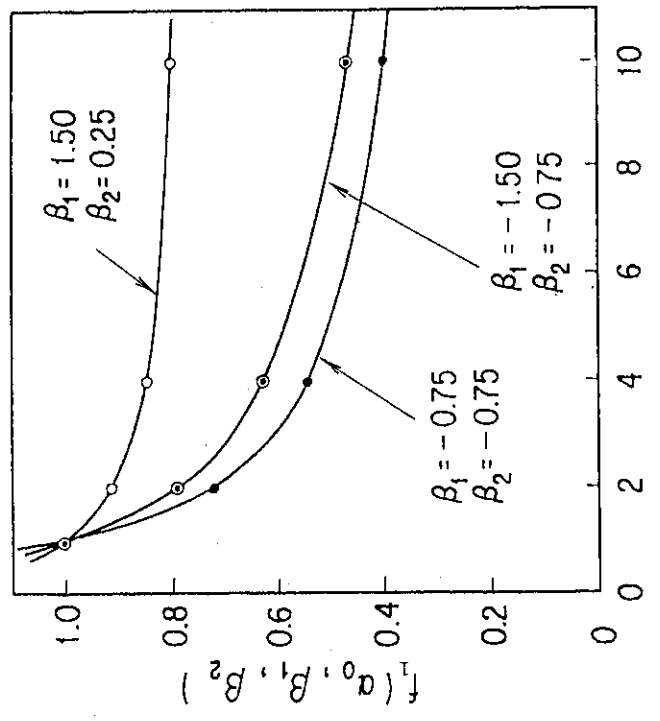

Fig. 1 $f_1(\alpha_0, \beta_1, \beta_2)$ as a function of α_0^{-1} with fixed β_1 and β_2

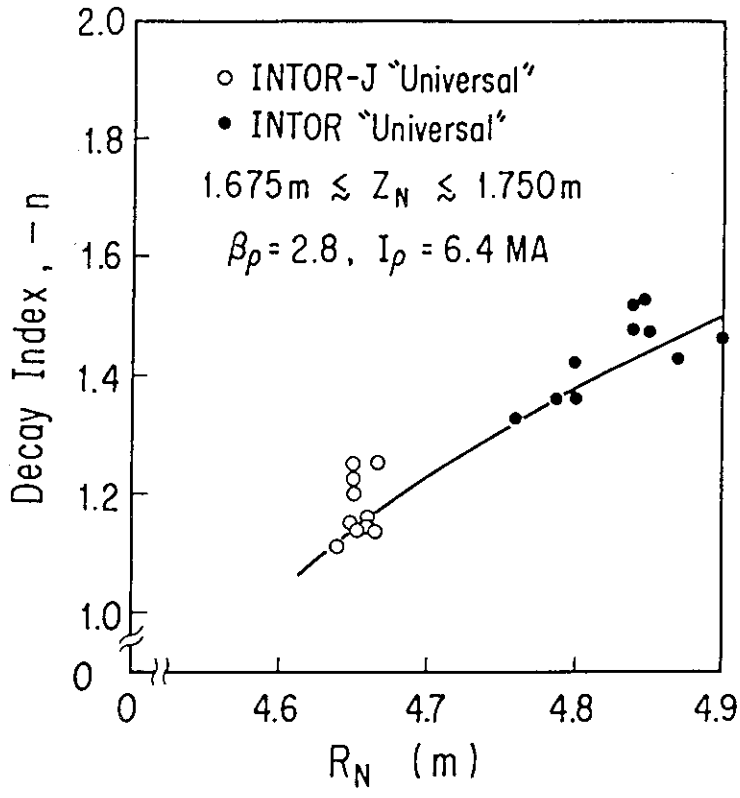

Fig. 3 Dependence of decay index , n upon the radial coordinate , R_N , of active null point in cases of both of the INTOR-J "Universal" and the INTOR "Universal"

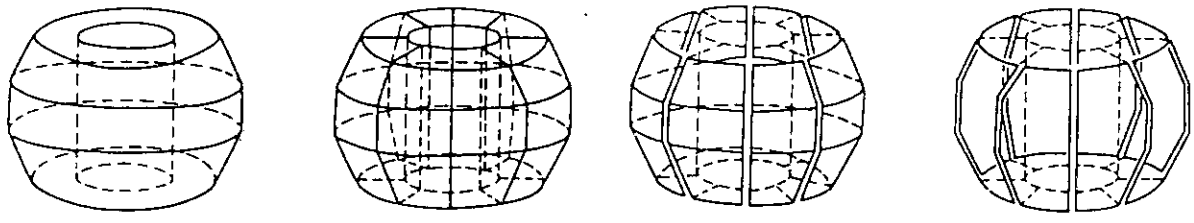

Fig. 4 Various types of shell-structures ; (a) doughnut without cuts, (b) doughnut with cuts , (c) plane ring with cuts , and (d) rectangular coils. These cross-section is shown in Fig. 5

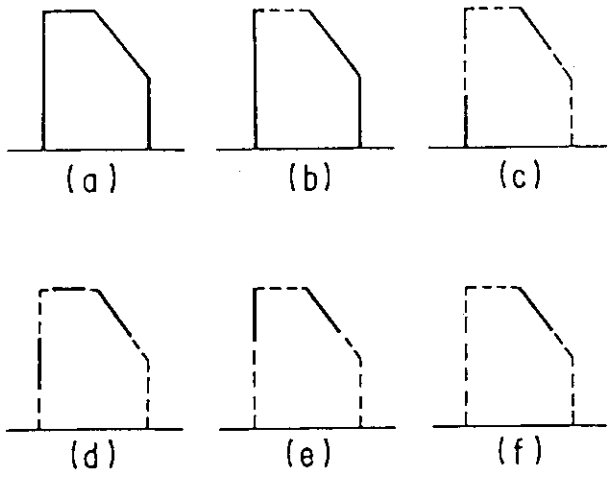

Fig. 5 Various types of plane ring shell-structures. Solid line means plane ring. Coordinates of A is (3.8,0.0) , B(6.6,0.0) , C(6.6,0.9) , D(5.8,2.2) , and E(3.8,2.2)

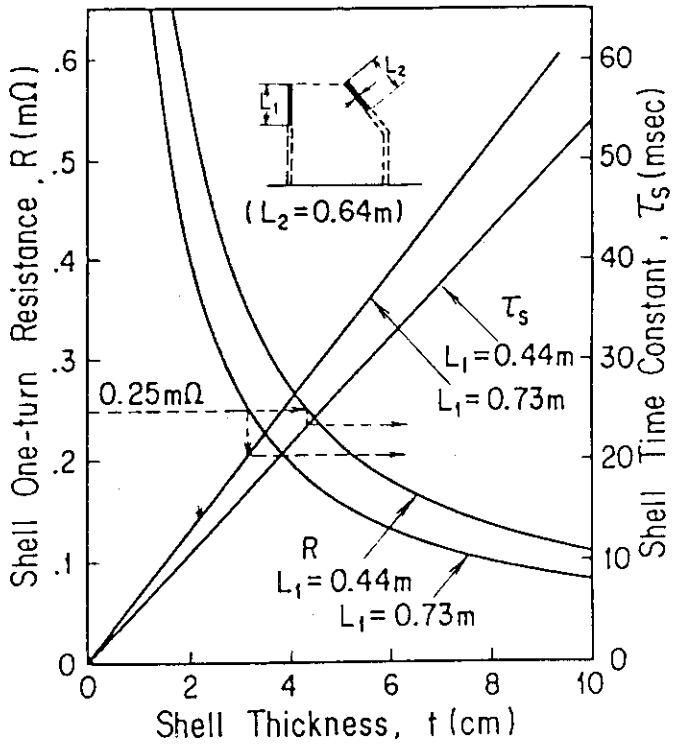

Fig. 6 One-turn resistance and time constant of shell-structure as a function of its thickness in case (e) of Fig.5. Material of the shell-structure is stainless steel with $7 \times 10^{-7}\ \Omega$ m in resistivity

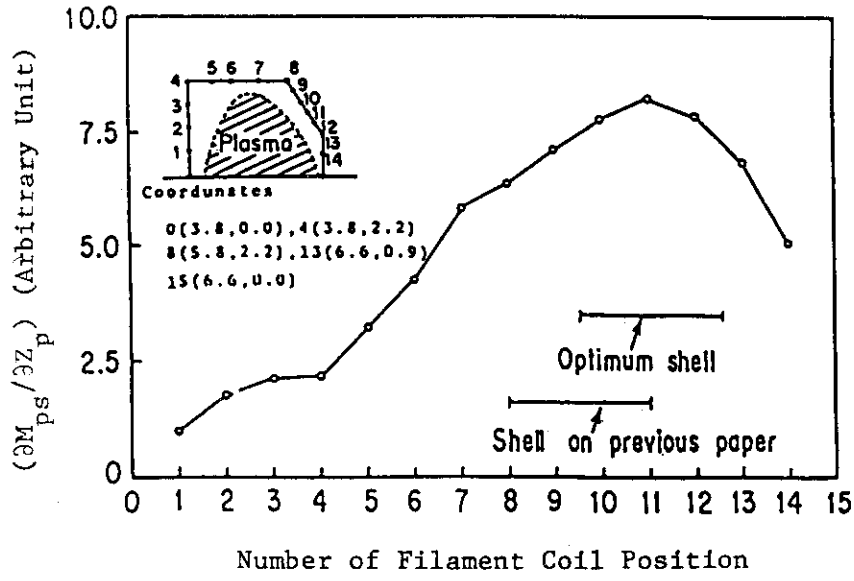

Fig. 7 Dependence of $(\partial M_{ps}/\partial Z_p)$ upon the location of filament current along the inner surface of plasma vessel

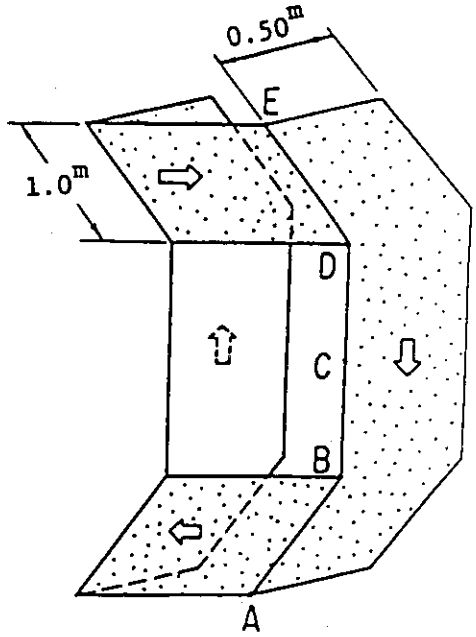

A (6.06m , - 1.77m) , B (6.60m , - 0.90m) ,

C (6.60m , 0.0m) , D (6.60m , 0.90m) ,

E (6.06m , 1.77m)

⇦ : Current Flow

Fig. 8 Structure of a new rectangular shell

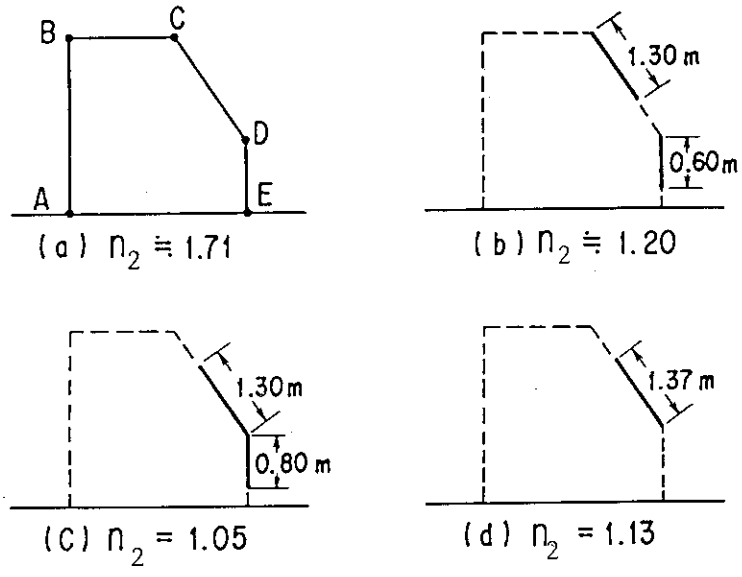

Fig. 9 Various types of plane ring structures located on the contour II. Coordinates of A is (3.8,0.0) , B(3.8,2.7) , C(5.8,2.7) , D(7.1,1.0) , E(7.1,0.0).

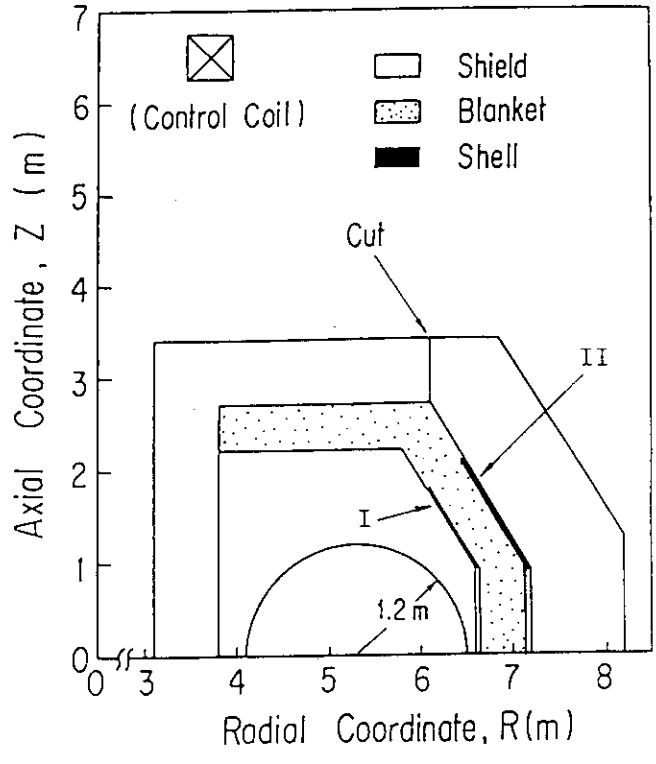

Fig. 10 Vertical cross-sectional view of inductive components used for the modelled feedback control system.

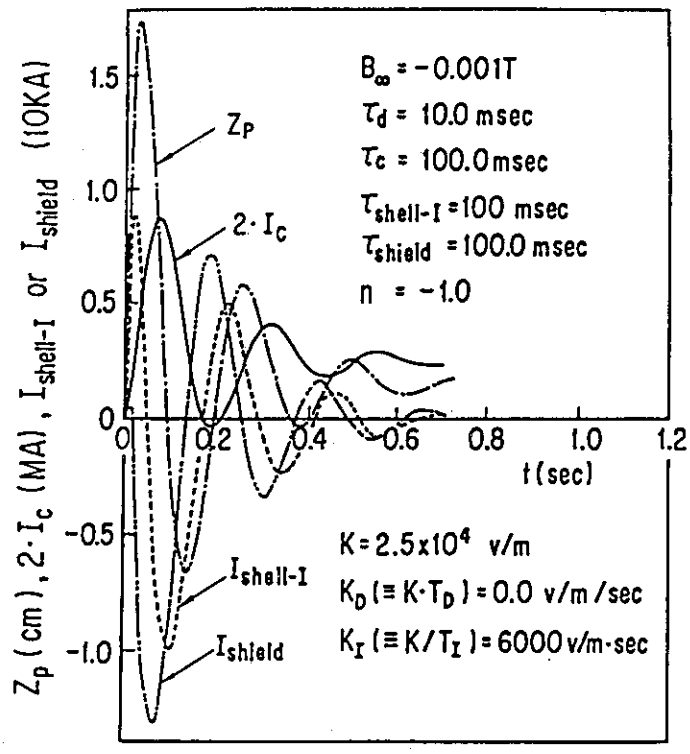

Fig.11 Typical time evolutions of Z_p, I_c, $I_{shell-I}$ and I_{shield} with the PI controler in case of the system(1)

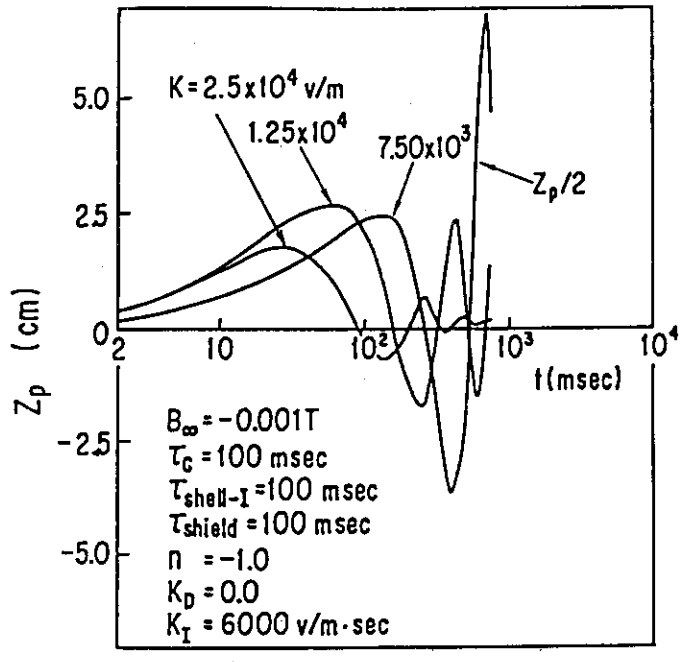

Fig.12 Time evolutions of Z_p for various K with the PI controller in case of the system(1)

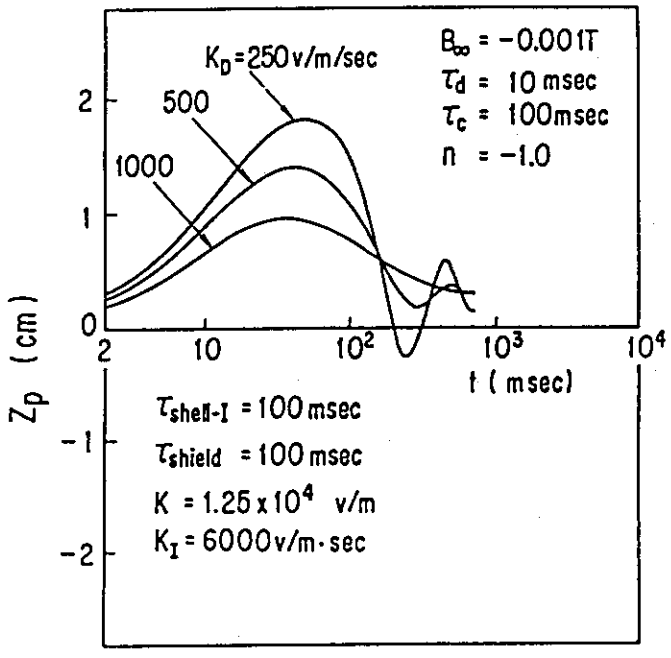

Fig. 13 Time evolutions of Z_p for various K_D with the PID controller in case of the system(1)

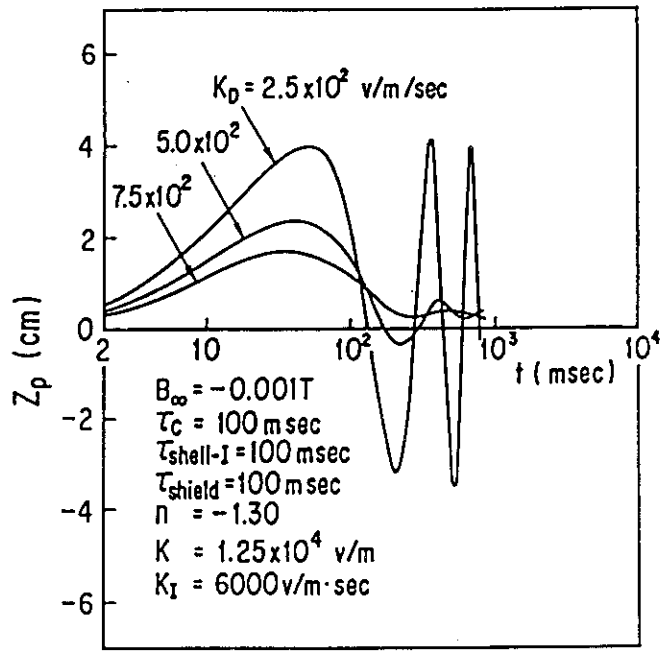

Fig. 14 Time evolutions of Z_p for various K_D with the PID controller in case of the system(1)

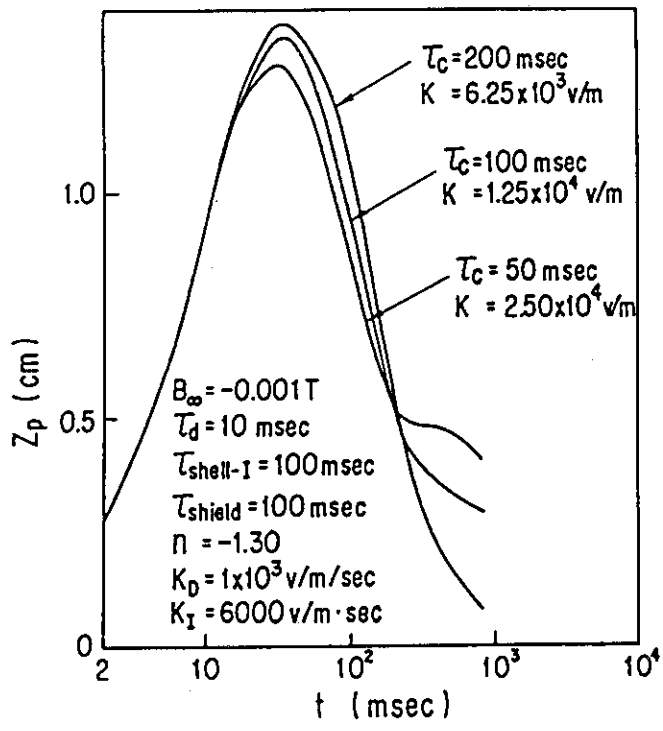

Fig.15 Time evolutions of Z_p on keeping $\tau_c \cdot K$ (=1.25 $\times 10^6$V·msec/M) constant with the PID controller in case of the system(1)

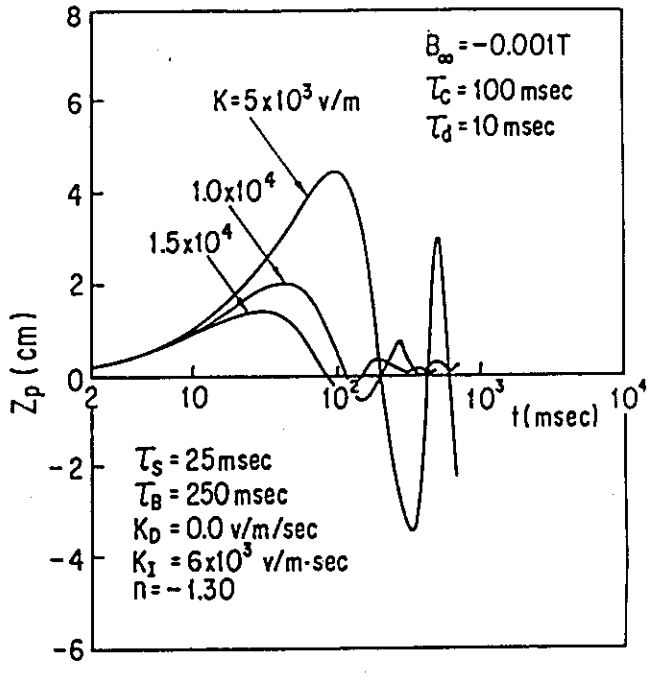

Fig.16 Time evolutions of Z_p for various K with the PI controller in case of the system(2)

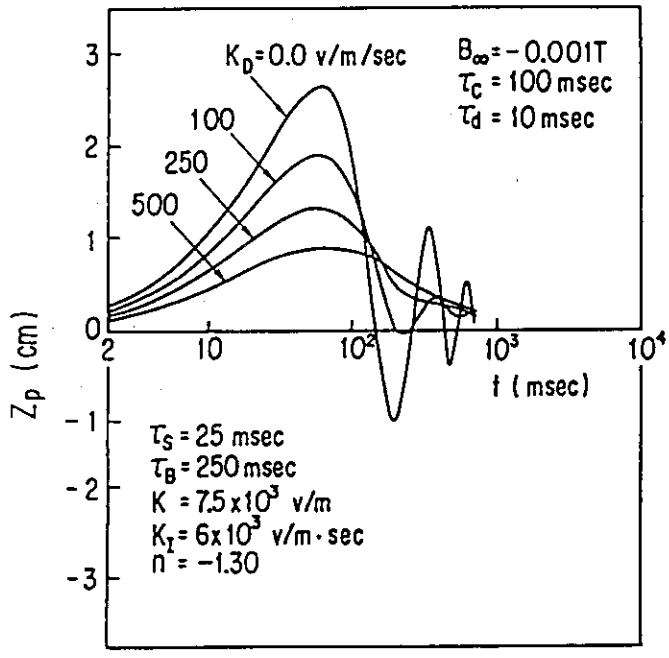

Fig.17 Time evolutions of Z_p for various K_D with the PID controller in case of the system(2)

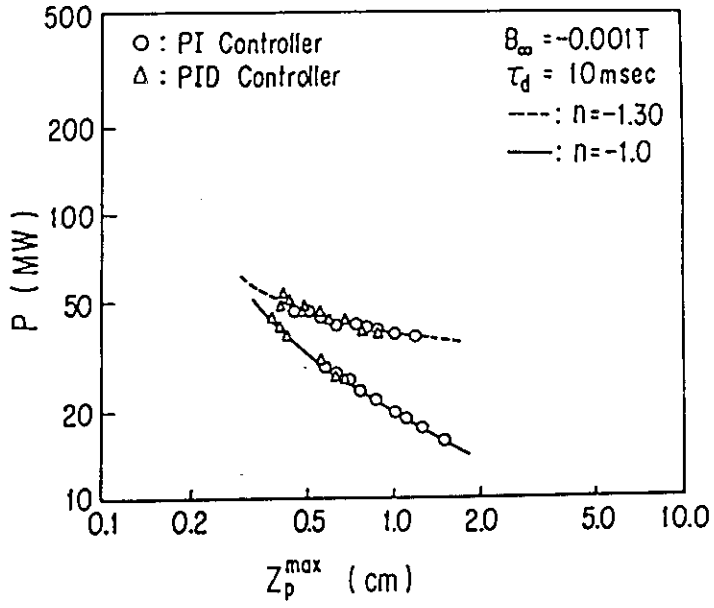

Fig.18 Dependence of the power , P ,required for the suppression and control of vertical instability upon the maximum vertical displacement , Z_p^{max}, obtained under the disturbance field ; $B = B_\infty \cdot (1.0 - \exp(-t/\tau_d))$, in case of the system(2)